REPRODUCTION
RESEARCH

Inhibition of zygotic DNA repair: transcriptome analysis of the offspring in trout (*Oncorhynchus mykiss*)

C Fernández-Díez, S González-Rojo, J Montfort[1], A Le Cam[1], J Bobe[1], V Robles, S Pérez-Cerezales and M P Herráez

Department of Molecular Biology, Faculty of Biology, University of León, Campus Vegazana s/n, León 24071, Spain and [1] INRA UR1037, Fish Physiology and Genomics, Rennes, France

Correspondence should be addressed to M P Herráez; Email: paz.herraez@unileon.es

Abstract

Zygotic repair of the paternal genome is a key event after fertilization. Spermatozoa accumulate DNA strand breaks during spermatogenesis and can suffer additional damage by different factors, including cryopreservation. Fertilization with DNA-damaged spermatozoa (DDS) is considered to promote implantation failures and abortions, but also long-term effects on the progeny that could be related with a defective repair. Base excision repair (BER) pathway is considered the most active in zygotic DNA repair, but healthy oocytes contain enzymes for all repairing pathways. In this study, the effects of the inhibition of the BER pathway in the zygote were analyzed on the progeny obtained after fertilization with differentially DDS. Massive gene expression (GE; 61 657 unique probes) was analyzed after hatching using microarrays. Trout oocytes are easily fertilized with DDS and the high prolificacy allows live progeny to be obtained even with a high rate of abortions. Nevertheless, the zygotic inhibition of Poly (ADP-ribose) polymerase, upstream of BER pathway, resulted in 810 differentially expressed genes (DEGs) after hatching. DEGs are related with DNA repair, apoptosis, telomere maintenance, or growth and development, revealing a scenario of impaired DNA damage signalization and repair. Downregulation of the apoptotic cascade was noticed, suggesting a selection of embryos tolerant to residual DNA damage during embryo development. Our results reveal changes in the progeny from defective repairing zygotes including higher malformations rate, weight gain, longer telomeres, and lower caspase 3/7 activity, whose long-term consequences should be analyzed in depth.

Reproduction (2015) **149** 101–111

Introduction

Recent studies have changed our perception of the contribution of sperm chromatin in early embryo development. The differential gene packaging in the spermatozoa, as well as the presence of epigenetic marks in specific genes at both histone and DNA levels, point to an essential role of the paternal chromatin in the genetic control of the first events occurring after fertilization (Carrell & Hammoud 2010, Speyer *et al*. 2010, Ward 2010). Fertilization with DNA damaged spermatozoa (DDS) is considered as an important factor leading to implantation failures and abortions both in mammals (Lin *et al*. 2008, Zini *et al*. 2008, Speyer *et al*. 2010) and fish (Ciereszko *et al*. 2005, Perez-Cerezales *et al*. 2010*a*). In addition, DDS has been related with later paternal effects such as abnormal weight at birth, higher susceptibility to certain diseases, or even premature aging (Evenson & Wixon 2006, Bowdin *et al*. 2007, Fernandez-Gonzalez *et al*. 2008, Barroso *et al*. 2009, Lim *et al*. 2009, Zini & Sigman 2009, Schulte *et al*. 2010, Zini 2011). Apart from intrinsic factors acting during spermatogenesis, many external agents, such as those produced by cold or frozen storage, could promote DNA injury in the ejaculate, being most of them related with the generation of reactive oxygen species (ROS; Evenson & Wixon 2006, Thomson *et al*. 2009, Perez-Cerezales *et al*. 2010*a*). Spermatozoa have a very limited capacity to repair DNA damage (Smith *et al*. 2013) and easily accumulate DNA lesions. DNA repair capacity declines during the latter part of spermatogenesis, and this function relies on the oocyte after fertilization. Therefore, repair of the paternal DNA takes place mainly in the zygote and during early developmental stages, being dependent on the mRNAs and proteins stored in the oocyte and on genes expressed very early in development (Derijck *et al*. 2008, Jaroudi *et al*. 2009). Mammalian oocytes express genes involved in all DNA repair pathways, as revealed in the transcriptome analyses performed at different stages of maturation providing the regulatory machinery required to avoid transmitting mutations into the next generation until the embryo genome is fully activated. Fertilization of oocytes from female mice defective in DNA repair machinery has demonstrated that this is a key factor in

ISSN 1470–1626 (paper) 1741–7899 (online)
DOI: 10.1530/REP-14-0382
Online version via www.reproduction-online.org

ensuring the genomic integrity of the conceptus (Marchetti *et al*. 2007, Derijck *et al*. 2008). Nevertheless, this ability to repair is limited. Yamauchi *et al*. (2007) observed the inability of the zygote to repair such damage after ICSI with DNA cleaved in 50 kb fragments. Moreover, DNA repair could, in turn, introduce new mutations depending on the kind of DNA damage and on the active repairing pathway. Therefore, as Gonzalez-Marin *et al*. (2012) stated, the effect of sperm DNA fragmentation on the offspring depends on the combined effects of sperm chromatin damage and the capacity of the oocyte to repair it.

Among the damages promoted in spermatozoa chromatin during cold or cryo-storage, oxidization of bases and the production of simple- and double-strand breaks (ssDNA and dsDNA respectively) are frequently reported. Shortening of spermatozoa telomeres has also been reported after cryopreservation of trout sperm (Perez-Cerezales *et al*. 2011). Oxidized bases and simple-strand breaks are repaired by the base excision repair (BER) pathway (Mitra *et al*. 2001). Double-strand breaks can, in turn, be repaired either using the homologous end-joining (HR) or non-homologous end-joining (NHEJ) pathways (Hilton *et al*. 2013), both of them operative during the zygotic cell cycle in mouse (Marchetti *et al*. 2007, Derijck *et al*. 2008) and zebrafish (Bladen *et al*. 2005). One of the signaling enzymes upstream the BER pathway is the poly(ADP-ribose) polymerase (PARP), catalyzing the so-called 'PARylation', the post-translational addition of ADP-ribose chains to a wide range of substrates, including the same PARP. Its role in DNA signaling and repair is well known and its inhibition generates an increase in double-strand breaks, leading to genetic instability (Beneke 2012, Lovato *et al*. 2012, Metzger *et al*. 2013). PARP activity has also been strongly suggested in dsDNA repair in the zygote (Matsuda & Tobari 1989). PARP inhibition is currently being used to promote cytotoxicity (Lovato *et al*. 2012, Hilton *et al*. 2013) being 3-aminobenzamide (3AB) one of the classical inhibitors.

Teleost are external fertilizers and pose a weak spermatic selection process, providing DDS with higher chances of fertilizing than in mammals (Perez-Cerezales *et al*. 2010*b*). Artificial fertilization procedures are easy to perform and, given their high fecundity, large progenies are obtained from the same mating. In addition, the external embryo development gives access to the embryos at any developmental stage, all these factors make fish a good model to analyze the role of sperm chromatin and oocyte repair in the reproductive outcome. In a previous study by our team (Perez-Cerezales *et al*. 2010*a*), we analyzed in *Oncorhynchus mykiss* the reproductive outcome of sperm carrying different levels of DNA fragmentation in trout and the effect of the zygotic inhibition of PARP. Our results revealed that fertilization rates decreased in batches fertilized with DDS according to the sperm fragmentation ratio, and embryo loss rates increased more significantly. Surprisingly, PARP inhibition did not affect fertilization rates and led to increased embryo loss in batches fertilized with high DDS, but not in those fertilized with intermediate degree DDS, revealing that the increase in genetic instability promoted by the inhibitor was only critical for the most susceptible embryos. This previous work indicates that the embryo has a high capacity to repair paternal DNA damage, estimated in a 10% of fragmented chromatin, as well as a high capacity to do this regardless of PARP activity.

A more in-depth analysis of larvae resulting from this fertilization procedure, able to progress within development and to successfully hatch, could help in the understanding of the extent of later effects of repairing activity on the offspring. In this study, we examined the possible consequences of PARP inhibition in the *O. mykiss* progeny by analyzing the transcriptome of 1-day-old larvae obtained by spermatozoa carrying different degree of DNA damage, as well as the effects of defective repair on the larvae performance.

Materials and methods

Reagents

All media components were purchased from Sigma–Aldrich except when otherwise stated.

Table 1 List of primers for gene expression.

Primer name	Primer set	Annealing Tm (°C)	Accession number	Amplicon size (bp)
ptges3	F: CCAGCGACTGCTAAGTGGTATG	55	BT073211.1	62
	R: TCCCCTACGCAGAACTCGAT	55		
Myc	F: TTGCTGTCCACTCCTCCTC	60	EU086537.1	197
	R: AACCCGCTCCACATACAGTC	60		
sumo1	F: GGTCAGGACAACAGCGAAAT	61	NM001160594.1	175
	R: CCTCATCTTCCATTCCAAGC	61		
e2f4	F: CAGACACCTCCTGCACTGAA	60	NM001140310.1	241
	R: CGGAGGAGTGGAGAGAACAC	60		
hint2	F: GGTCACCTCCTAGTGGTTGC	64	NM001165053.1	158
	R: TAACCTGGAGGCCAGTTCAG	64		

Sequences start from 5′ to 3′. Annealing temperature, accession number and amplicon size are specified for each pair of primers.

Table 2 Nucleotide sequences of the PCR primers used to assay the telomere length by real-time quantitative PCR.

Primer name	Primer set	Source
Telomere	F: CGGTTTGTTTGGGTTTGGGTTTGGGTTTGGGTTTGGGTT R: GGCTTGCCTTACCCTTACCCTTACCCTTACCCTTACCCT	Pérez-Cerezales *et al.* (2011)
18S ribosomal DNA	F: CGGAGGTTCGAAGACGATCA R: TCGCTAGTTGGCATCGTTTAT	Pérez-Cerezales *et al.* (2011)

Sequences start from 5′ to 3′.

Experimental procedure

The experiments were carried out in accordance with European Union Council Guidelines (86/609/CEE), following Spanish regulations (BOE 67/8509-12, 1988) for the use of laboratory animals, and were approved by the Scientific Committee of the University of León.

Larvae were obtained from fertilization procedures performed previously as described in Perez-Cerezales *et al.* (2010*a*). Briefly, fresh sperm and eggs were obtained from four males and two female rainbow trout (*O. mykiss*) from Las Zayas fish-farm (León, Spain). Fish were maintained under natural photoperiod, and gametes were obtained during the natural reproductive season (January–February, with a 6–8 °C water temperature). The sperm were collected by cannulation and their motility was checked by visual inspection using light microscopy. All samples scored more than 90% motile spermatozoa. The oocytes were extracted by stripping from females anesthetized with MS222. The eggs were pooled and divided into 200 egg batches for fertilization trials.

Immediately after collection, sperm from each male was divided into three aliquots: one used as fresh control (F samples) and two frozen in 0.5 ml French straws using different additives in the extender. For freezing, sperm was diluted 1:3 (sperm:extender) in #6 from Erdahl and Graham (0.7 mM $CaCl_2 \times 2H_2O$, 1.08 mM $MgCl_2 \times 6H_2O$, 1.49 mM Na_2HPO_4, 34.30 mM KCl, 100 mM NaCl, 0.52 mM citric acid, 55.5 mM glucose, 4.52 mM KOH, 6.48 mM bicine, and 323 mOsm/kg, pH 7.4) containing 7% Me_2SO (v/v) as a permeable cryoprotectant and either 10% (v/v) egg yolk (EY samples) or 12% (w/v) (LDL samples) as a membrane protector. LDL was obtained following the protocol described previously (Moussa *et al.* 2002). DNA fragmentation was evaluated in fresh and frozen/thawed sperm using the comet assay as described previously (Perez-Cerezales *et al.* 2011).

Egg batches were fertilized with sperm from each male using fresh sperm diluted 1:3 (sperm:extender) in #6 from Erdahl and Graham, or sperm cryopreserved with egg yolk, or LDL. Four batches of 200 eggs were fertilized for each experimental condition (2400 eggs/male). Ten minutes later, the eggs were washed with water and two batches of each treatment were incubated in the dark, for 6 h at 10 °C in 15 mM 3AB to inhibit the PARP activity (two batches per treatment) or in water (two batches per treatment). Then, the eggs were washed with water and incubated in the dark, at 10 °C and with a continuous water flow until hatching. The fertilization rate was calculated over a subsample of 30 embryos extracted from each batch at blastula stage to evaluate embryo development. One day after hatching, ten live larvae from each batch were taken and frozen at −80 °C for RNA extraction.

Total RNA extraction

Total RNA was obtained using a Trizol Reagent kit (Applied Biosystems) following the manufacturer's instructions. RNA integrity was checked with the Agilent Bioanalyzer (Agilent Technologies, Massy, France) and the yield was estimated using a Nanodrop ND-1000 spectrophotometer (Labtech, Palaiseau, France). Total RNA was stored at −80 °C until its processing.

GE microarrays processing

RNA from ten larvae from each batch was pooled, therefore four samples (corresponding to the progeny from each male) were analyzed per treatment (sperm type and fertilization/incubation procedure). Rainbow trout GE profiling was performed using an Agilent 8×60 K high-density oligonucleotide microarray (GEO platform #GPL15840). The 8×60 K Rainbow trout Microarray design was done using eArray (an Agilent freeweb-based application). Each area of the slide contains 62 976 features. Among those 62 976 features, 61 657 are unique probes (with a hit on Swiss-Prot Database) and the 1319 remaining features are controls. Several probes can match for a same gene. Labeling and hybridization steps were performed following the 'One-Color Microarray-Based GE Analysis (Low Input Quick Amp labeling)' Agilent protocol. For each sample, 150 ng total RNA were amplified and labeled using Cy3-CTP. Yield (>0.825 ng cRNA) and specific activity (>6 pmol of Cy3/μg of cRNA) of Cy3-cRNA produced were

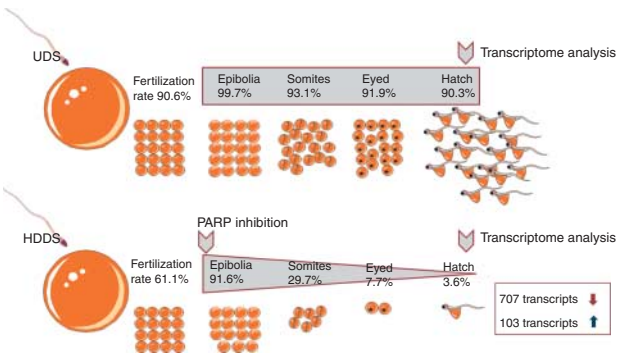

Figure 1 Schematic representation of the experimental procedure and the survival rates at different stages after fertilization in the most extreme treatments: fertilization with undamaged sperm (USD) and incubation under normal conditions, or fertilization with highly damaged sperm (HDDS) (frozen with egg yolk) followed by inhibition of the Base Excision Repair Pathway (PARP inhibition). Red and blue arrows represent down- or up-regulated transcripts in larvae obtained after PARP inhibition respectively.

checked with the Nanodrop: 600 ng of Cy3-cRNA was fragmented and hybridized on each array. Hybridization was carried out for 17 h at 65 °C in a rotating hybridization oven before washing and scanning with an Agilent Scanner (Agilent DNA Microarray Scanner, Agilent Technologies) using the standard parameters for a GE microarray (channel: green, resolution: 5 µm, TIFF: 20 bits). Data were then obtained using the Agilent Feature Extraction Software (10.7.3.1). Before analysis, saturated spots, non-uniform spots, and spots not significantly different from background ($k=5$) were flagged using the Agilent Gene-spring GX Software (10.5.0). The probes were considered valid when corresponding spots remained present in at least 80% of the replicates of each experimental condition after the flagging procedure. Data were subsequently scale-normalized using the median value of each array.

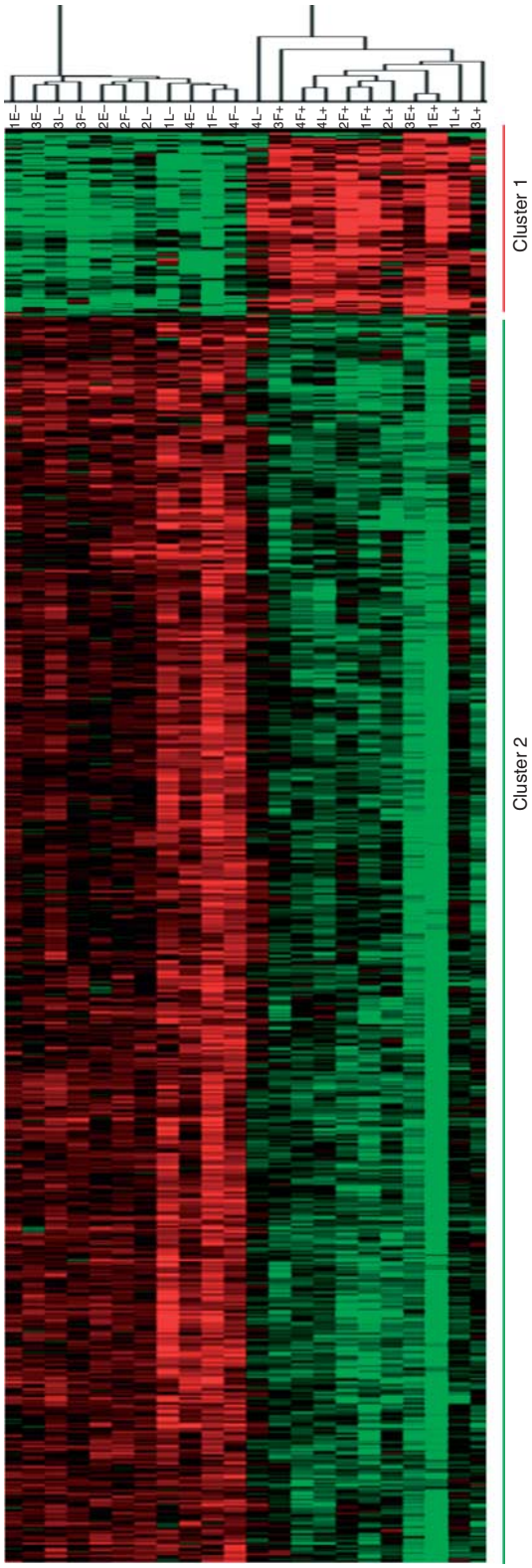

Gene ontology analysis

Gene ontology was performed using DAVID Bioinformatics Resources v6.7 to explore functional annotation (Huang da *et al*. 2009). Gene names of differentially expressed gene (DEG) and total microarray genes were both imported into the web-software as gene list and background list respectively. In order to show functional classification, clustering annotation was used and a threshold score of 5 was applied (Supplementary File 2, see section on supplementary data given at the end of this article).

q-PCR validation

The differential expression of five genes from those with higher sequence similarity with *O. mykiss* annotations, implied in cell cycle control (*e2f4* and *sumo1*), mitochondrial activity (*hint2*), maintenance and regulation of telomere length (*myc* and *ptges3*), morphogenesis (*myc*), DNA repair pathways (*sumo1*), and apoptosis (*sumo1*), was validated by q-PCR.

Total RNA (1 µg) was reverse transcribed using the High Capacity cDNA Kit (Applied Biosystems) following the manufacturer's instructions. The conditions applied for reverse transcription were 25 °C for 10 min, 37 °C for 120 min, and final extension at 85 °C for 5 min. Real-time PCR was performed using a Step-One Plus thermocycler (Applied Biosystems). Reverse transcription products were diluted 1: 3 and 2 µl were used for each q-PCR. The primers for q-PCR were designed using Primer Express (Software v2.0, Applied Biosystems) and Primer Select (Software v10.1 DNA Star, Lasergene Core Suit). The primer nucleotide sequences and annealing temperature from rainbow trout related transcripts can be found in additional material (Table 1). The q-PCR conditions were optimized for the different primers to achieve similar amplification efficiencies. Product specificity was tested by melting curves and product size was visualized by electrophoresis on agarose gel (data not shown).

Figure 2 Image provided by cluster analysis showing the expression profiles of the transcriptome in the larvae progenies of rainbow trout (*Oncorhynchus mykiss*) 1 day after hatch. Cluster 1 shows 103 probesets with a higher expression in batches treated with 3AB, PARP inhibitor. Cluster 2 represents 717 probesets with a lower expression in the same batches. Letters and numbers identify the batches: numbers identify the male used for fertilizing; (+/−) batches incubated with/without (3AB); E: sperm cryopreserved with egg yolk; L: sperm cryopreserved with LDL and F: fresh sperm.

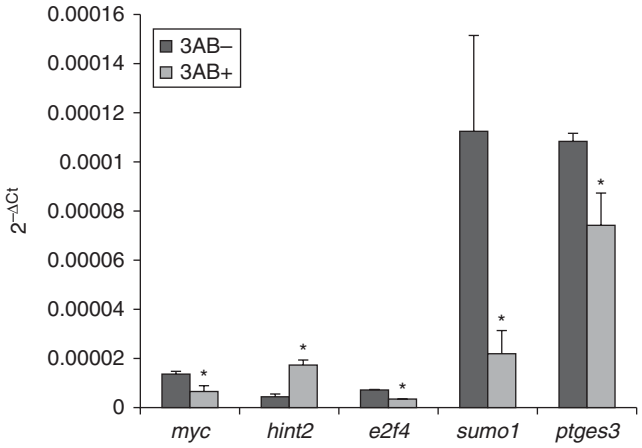

Figure 3 mRNA levels (fold change: $2^{-\Delta Ct}$) for *myc*, *hint2*, *e2f4*, *sumo1*, and *ptges3* at 1 dph from trout larvae obtained after normal artificial fertilization or after zygotic inhibition of BER DNA repair pathway using 3AB. Data represent mean values ± S.D. ($n=40$). Asterisks show significant differences between treatments ($P<0.05$).

Reaction mixtures (total volume 20 µl) contained 2 µl of cDNA, 10 µl of 1× SYBR Green Master mix (Applied Biosystems), and 2 µl of 500 nM each forward and reverse primer. q-PCR was initiated with a pre-incubation phase of 10 min at 95 °C followed by 40 cycles of 95 °C denaturation for 10 s and the temperature for primer extension for 1 min. Three technical replicates were done per sample.

Expression level for each transcript was normalized to 18S gene using the delta-Ct ($2-\Delta Ct$) method (FoldChange) to analyze relative changes in GE concerning the housekeeping expression.

Offspring evaluation

After the evaluation of GE, progenies from four males were obtained with and without inhibition of the BER pathway following the same procedure above previously. Next, parameters were analyzed in the offspring obtained from both types of fertilization: percentage of malformations one day post hatching (1 dph), weight 1 and 30 dph, telomere length, apoptotic activity (activity of caspases 3–7), and ploidy.

Telomere length was measured in larvae 1 dph. Genomic DNA extraction was performed using the protocol described by our group (Cartón-García *et al.* 2013), including a previous step of larvae digestion with 6 mg/ml collagenase 2 h at 37 °C. To stop the reaction, the cells were washed with two volumes of PBS and the pellet was resuspended in 700 µl of extraction buffer (10 mM Tris–HCl, pH 8.0; 100 mM EDTA, pH 8.0; 0.5% (v/v) s SDS, supplemented with 0.5 µl proteinase K (1 mg/ml)). DNA quantity and yield were determined spectrophotometrically at 260 nm (Nanodrop ND-1000 Spectrophotometer, Thermo Scientific, Waltham, MA, USA). All samples showed high purity (A260/A280 >1.8).

Total genomic DNA was used for measuring telomere length by real-time PCR assay, as described previously (Perez-Cerezales *et al.* 2011). PCRs were performed using telomeric primers and primers for 18S ribosomal DNA as housekeeping gene (Table 2). The telomere signal was normalized dividing by the signal of 18S DNA, the average of this ratio was reported as relative telomere length in comparison with control larvae.

To analyze the apoptotic activity, ten larvae per batch were anesthetized with MS-222 (80 mg/l) and cut in small pieces. Larvae fragments were incubated 3 h under agitation in a dissociation solution containing 3.6% trypsine, 2.4 µl DNAse I (Applied Biosystems), and 10% FBS in Leibovitz's (L-15) medium. The larvae fragments were gently and repeatedly pipetted to facilitate the dissociation process. Then, cells were filtered by 140 µm nylon mesh and washed twice with a solution containing L-15 medium. The activity of caspases 3/7 was analyzed using the Caspase-Glo 3/7 Assay Systems Kit (Promega) following the instructions of the manufacturer.

Ploidy analysis was performed with somatic cells extracted from the gills of 30 dph larvae, following the protocol described by Zhang & Arai (1996). The cells were labeled with propidium iodide (PI) and DNA content was evaluated by flow cytometry using a FACScalibur (Becton Dickinson, San Diego, CA, USA) cytometer adjusted for blue excitation (488 nm) line for the detection of PI (670/30). A total of 10 000 events were acquired per sample and data were analyzed using the Weasel 3.1 free software. Nuclear DNA content was expressed as DNA index (DI), the ratio between median G0/G1 peak of control and treated larvae.

Data analysis

To identify DEGs among treatments, a two-way ANOVA was performed using Genespring GX Software. A Benjamini–Hochberg correction was applied (FDR cut off <0.005). Hierarchical clustering analysis was performed on genes and samples using Cluster and Tree View softwares (Eisen *et al.* 1998) using the following parameters: median-centered (genes), Pearson correlation, and average linkage. For annotation, blastX was performed on Swissprot database and the best blast hit was chosen (*e*-value $<5\times10^{-2}$ with a minimum id of 85%).

Significant differences in GE, and all the parameters analyzed in the progeny, were validated by an unpaired *t*-test using the GraphPad Prism v5.0 Software, San Diego, CA, USA (*P* value <0.05).

Results

Spermatozoa DNA fragmentation, fertility rates, and hatching rates were shown as reported by Perez-Cerezales *et al.* (2010*a*) and some results are summarized in Fig. 1.

Table 3 Expression patterns on rainbow trout larvae progenies from zygotes incubated with or without the inhibitor of PARP.

	Incubated without 3AB				Incubated with 3AB			
	♂1	♂2	♂3	♂4	♂1	♂2	♂3	♂4
Fresh	N	N	N	N	A	A	A	A
EY	N	N	N	N	A	NH	A	NH
LDL	N	N	N	A	A	A	A	A

♂ Male used for fertilization. Fresh, fresh sperm; EY, cryopreserved sperm with egg yolk; LDL, cryopreserved sperm with LDL; N, normal pattern; A, altered pattern; NH, no hatching.

Table 4 Differentially expressed probesets with unique gene name involved in cell cycle.

G1/S, S and G2/M	Cell cycle checkpoints and cell cycle arrest	Mitosis	Others
upf1[a]	*atm*	*cenpk4*	*fgfr4*[a]
anapc11	*triap1b*	*mms19*	*ccnl*
e2f4	*mad2*	*haus2*	*e2f4*
khdrbs1	*spc25*	*stmn3*	*mapksp1*
ube2	*spc22*	*titin*	*rad51*
znf473	*ppm1l*	*cenpa*	*triap1b*
pole		*exo1*	*kiaa0892*
khdrbs1		*dusp13*	*npm1*
Ing4			*Cetn2*
			Cetn1
			Cetn3
			smarca4
			cenpj
			ube2e1
			psme3
			psmd6
			psma1
			psma2
			psma3
			psma7
			psma6
			myc
			cdc42
			vps4
			erh
			pa2g4
			pfdn1
			fnta
			chmp1b

[a]Transcripts with a higher expression in larvae with the 'altered' expression profile (*FDR* <0.005).

Corresponding data were deposited in GE Omnibus database (GEO Series accession number GSE52217). Out of the 61 657 probes, 810 features showed a significant differential expression (FDR cut off <0.005) (Supplementary Table 1, see section on supplementary data given at the end of this article).

The clustering analysis of these 810 probesets (Fig. 2) allowed two major clusters of genes to be identified. The first cluster included 103 probesets (given in Supplementary Table 2, see section on supplementary data given at the end of this article) that were upregulated in larvae obtained after fertilization and incubation with 3AB during the first cleavage. In contrast, the second cluster included 707 (Supplementary Table 3) downregulated probesets in the same batches. The expression analysis of the probesets by qPCR confirmed the differential expression provided by the array showing a downregulation of *myc*, *e2f4*, *sumo1*, and *ptges3* and upregulation of *hint2* with the inhibition of DNA repair (Fig. 3). The cluster analysis showed different expression patterns according to type of fertilization: the larvae obtained from standard artificial fecundation showed a normal profile, and the larvae obtained after incubation of fertilized eggs with the PARP inhibitor showed an altered profile (Table 3). The progenies from one male carrying DDS and non-treated with the inhibitor (Fig. 2 column 4L-) better clustered with batches showing the 'altered' profile, but with a very low *P* value (*P*=0.05806), displaying a much more reduced number of genes up- or down-regulated with respect to the normal pattern than the inhibited ones. Among the 810 DEG, 604 have a gene name, 553 being unique gene names. Among these 553 unique genenames, 370.correspond to at least one gene ontology (GO) biological process term and are included in nine different clusters according to cellular components, biological functions, or molecular processes (Suplementary file 4).

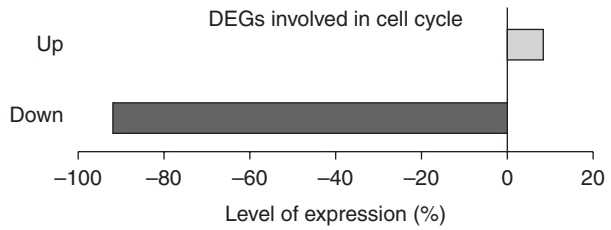

Figure 4 Percentage of (DEGs) with unique gene name involved in cell cycle process according to the up- or down-regulation after PARP inhibition.

Cluster 6 contains at least 52 genes (Table 4) related with the cell cycle control (92.3% of them downregulated; Fig. 4). All of these genes related with cell cycle checkpoints and arrest were downregulated in larvae hatched after the inhibition of the BER pathway.

Cluster 4 included at least 37 genes related with programed cell death (Table 5) and all the proapototic genes were downregulated after the inhibition of PARP activity (Fig. 5).

With regard to the control of the transcription mechanism two of the functional clusters (three and eight) aggregates an important number of genes, related with different pathways involved in morphogenesis, DNA repair, cell cycle, etc.

Among the 370 genes included in the nine GO clusters, at least 23 are involved in DNA repair (Table 6),

Table 5 Differentially expressed probesets with unique gene name involved in apoptotic activity.

Apoptotic process	Regulation of cell death		Execution	Signaling pathways	Others
	Positive	Negative			
ywhaz	*ing4*	*dnajb6*	*hmgb1*	*fis1*	*capn10*[a]
prkce[a]	*psenen*	*fas*	*madd*[a]	*psme3*	*tm2*
actn2[a]	*pdia3*	*angpt1*		*myc*[a]	*fxr1*[a]
fnta	*atm*	*psme3*		*madd*[a]	*rtn3*
actn3[a]	*btg1*	*igf1r*[a]		*ddx47*	*nckap1*
traf3		*madd*[a]		*pttg1*	*pdcd2*
		dad1		*triap1*	*trim69*
		triap1		*diablo*	*cln*
					npm1
					rpb2

[a]Transcripts with a higher expression in larvae with the 'altered' expression profile (*FDR* <0.005).

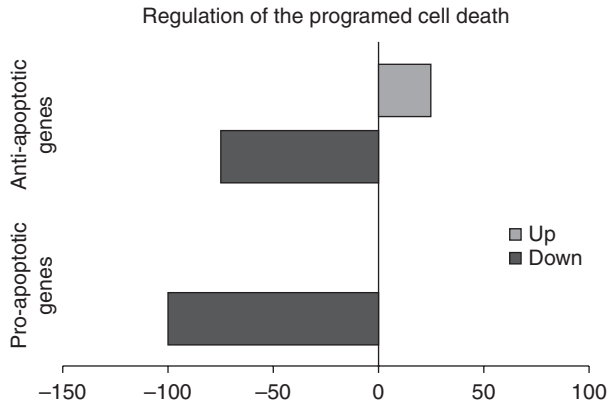

Figure 5 Percentage of DEGs with unique gene name involved in pro- or anti-apoptotic activity according to the up- or down-regulation after PARP inhibition.

most of them being downregulated in larvae with the altered profile. A number of DEGs are related with the control of telomere length (Table 7), only one of them showing upregulation in larvae with an altered profile, *terf1*, and the rest being downregulated. At least 64 DEGs were related with growth and development (Table 8). We found genes involved in the early embryo development control (symmetry, axis, segmentation, gastrulation, etc.), pluripotency maintenance, organogenesis, tissues differentiation, and nervous system development. Focusing on the mitochondrial process (Table 9), at least, 22 DEGs were found and all of them were downregulated.

The analysis of larvae showed that zygotic inhibition of DNA repair promoted a slight increase in the rate of larval malformations 1 dph, from 8.4 to 12.11% (Fig. 6A), mainly skeletal malformations and defective yolk sac. Larvae from inhibited batches showed an increased growth rate (66% weight gain from 1 to 30 dah in treated batches vs 59% in non-treated batches; Fig. 6B). Apoptosis was also affected by the treatment revealing a lower activity of caspases 3/7 in larvae from the treated animals (Fig. 6C), which also showed longer telomeres (Fig. 6D). All the treated larvae showed a DI = 1, indicating the same ploidy than control larvae (Fig. 7).

Discussion

Zygotic DNA repair is a process required to repair injuries in the paternal DNA, produced by intrinsic as well as external factors, which spermatozoa is exposed to, and which could accumulate during the final steps of spermatogenesis and beyond (Derijck *et al*. 2008). DNA repairing pathways are lesion specific, and, as was previously quoted, oocytes seem to have the required transcripts and proteins to activate all of them (Jaroudi & SenGupta 2007). The sperm used in this work for fertilization was analyzed by Perez-Cerezales *et al*. (2011), which contained different degrees of damage. Therefore, fertilization with the different sperm samples would require a different repairing effort in the zygote, and promote different degree of genetic instability in the obtained embryos. In fact, a higher loss rate of embryo was reported in frozen sperm batches, mainly with EY. Zygote seems to have the ability to effectively repair at least a 10% of fragmented paternal chromatin, because EY samples, carrying at least a 10% fragmentation in all the spermatozoa, generated normal progeny as reported by the same team (Perez-Cerezales *et al*. 2010*a*). Nevertheless, as revealed in the transcriptome analysis, once embryo development is completed, hatched larvae did not show great differences according to the kind of sperm used for fertilization and only one of the progenies obtained with damaged sperm showed an expression profile different from the one considered as 'normal' pattern in absence of DNA repair inhibition. This could reflect that most embryos carrying chromosomal or genetic aberrations from paternal origin are lost during development and does not progress to hatch, being survivors from the less damaged spermatozoa.

The maternal ability to repair paternal injuries thus seems to be very effective, but risk could arise when repairing pathways are impaired. It is well known that defective repair of single-strand breaks by the BER pathway results in an increase in double-strand breaks after replication (Hilton *et al*. 2013, Metzger *et al*. 2013). This is the basis for using PARP enzyme inhibitors such as 3AB in cancer therapy: PARP inhibition promotes failure in the BER pathway, increasing dsDNA, which are

Table 6 Differentially expressed probesets with unique gene name involved in DNA repair pathways: base excision repair (BER) pathway, nucleotid excision repair (NER) pathway, homologous recombination (HR), non-homologous end joining (NHEJ), double strand breaks (DSB) pathway, checkpoint ATM/ATR and, others.

BER pathway	NER pathway	HR pathway	NHEJ pathway	DSB pathway	ATM/ATR signaling	Others
apex1	*rad23*	*xrcc3*	*nono*	*atm*	*atm*	*exo1*
triap1b	*triap1b*				*triap1b*	*rad23*
	ube2b				*pttg1*	*xrcc3*
						pole
						hmgb1
						upf1[a]
						rpa
						rfc2
						asf

[a]Transcripts with a higher expression in larvae with the 'altered' expression profile (*FDR* <0.005).

Table 7 Differentially expressed probesets with unique gene name involved in maintenance and regulation of telomere length.

Maintenance	Regulation
terf1[a]	*terf1*[a]
atm	*myc*
hspb11	
myc	
ptges3	
rad23	
rfc2	
tcerg1	

[a]Transcripts with a higher expression in larvae with the 'altered' expression profile (*FDR* <0.005).

repaired using the HR or the NHEJ pathway. Tumor cells lacking functional HR system are forced to use the NHEJ pathway, accumulating genetic errors that promote cell death (Lovato *et al*. 2012, Hilton *et al*. 2013, Metzger *et al*. 2013). In our study, the use of 3AB immediately after fertilization was expected to generate an intense genetic stress, considering that first cell cycle lacking the G1-S checkpoint is able to arrest replication (Shimura *et al*. 2002) and then embryos will progress with cleavage. Moreover, transient double-strand breaks are also promoted during sperm chromatin remodeling after penetrating in the mouse oocyte (Bizzaro *et al*. 2000, Derijck *et al*. 2006). A high number of double-strand breaks should then be generated after PARP inhibition, particularly in the EY progeny. Nevertheless, PARP inhibition only increased the embryo loss rates in batches fertilized with the most highly damaged sperm (Perez-Cerezales *et al*. 2010*a*), demonstrating that only those batches were unable to repair the increased number of dsDNA. Apparently, the level of damage in F and LDL sperm was repaired by alternative pathways compatible with successful embryo development. The use of alternative pathways in addition to BER was confirmed in mice after ICSI with irradiated sperm carrying dsDNA. When oocytes from strains defective in the NHEJ or HR pathway for repairing double-strand breaks where fertilized by ICSI, the embryonic lethality significantly increased (Marchetti *et al*. 2007). Both pathways are active in the mammalian zygote, as was also demonstrated by Derijck *et al*. (2008) in a similar experience fertilizing with irradiated sperm oocytes from defective mouse. The inhibition of the NEHJ pathway in zebrafish using morpholines at 1 cell and 6 hpf also increased the apopototic activity and malformations rate, confirming in fish the importance of this alternative pathway (Bladen *et al*. 2005). Our results also suggest the ability of the oocyte to repair paternal damage by alternative pathways without introducing lethal genetic errors.

In spite of the ability to provide apparently normal progeny, massive differences in the transcriptome were caused by treatment with the inhibitor of PARP after fertilization. Considering that hatching took place 26 days after fertilization, PARP inhibition did not promote a transient modification of the repairing activity, but a long-term change in the regulation of different processes. The treated embryos could have required the activation of compensatory mechanisms to bypass the reduction in PARP activity and these changes produced a number of DEGs. Results showed that a wide range of DEGs involved in a variety of functions. Some of them are not known substrates of PARP neither are downstream PARP in known pathways, suggesting the activation or inhibition of alternative mechanisms. The expression level was modified (mostly downregulated) in transcripts involved in all DNA repairing pathways, suggesting changes in the regulation of the processes and

Table 8 Differentially expressed probesets with unique gene name involved in growth and development.

Axis/ symmetry/ segmentation	Embryo development	Gastrulation	Nervous system development	Morphogenesis/ tissues	Pluripotency/ cell differentation	Eye	Growth factors signaling	Others
nr2f2[a]	*wnt16*	*zbtb17*	*Dmd*[a]	*nr2f2*[a]	*fgfr4*[a]	*mab21l2*	*fgfr4*[a]	*ing4*
	id2		*myo1b*[a]	*Prkce*[a]	*smarca4*[a]	*actl6a*	*glg1*[a]	*triap1b*
	ube2b		*nptn*[a]	*angpt1*	*Vcan*[a]	*ephb2*	*igf1r*[a]	
	kif3a		*smarca4*[a]	*atm*	*vps37d*	*pknox1*	*Adipoq*	
	angpt1		*atm*	*myc*	*tspy2*	*mab21l2*	*Ptn*[a]	
	dad1		*hmgb1*	*tbca*	*btg1*		*sertad2*	
	hlx		*hlx*	*wnt16*	*hlx*		*fgffr4*	
			actl6a	*fhl1*	*fnta*		*e2f4*	
			hes5	*serp1*	*e2f4*		*fgfr4*	
			ephb2	*titin*	*ybx1*		nptn	
			tnr	*esrrb*	*esrrb*			
			cdc42	*vcan*	*angpt1*			
			dspp	*trappc2*	*pknox1*			
			hlx	*mab21l2*	*nus1*			
			eif2b	*hlx*	*btg1*			
				ppp2r1b	*itgv*			
				rab26	*rpl22*			
				jpk1	*ap3*			
				mesdc2				

[a]Transcripts with a higher expression in larvae with the 'altered' expression profile (*FDR* <0.005).

Table 9 Differentially expressed probesets with unique gene name involved in mitochondrial processes.

ATP production	Ribosomal proteins	Others
atp5g1	*mrpl32*	*hint2*[a]
atp5g3	*mrpl37*	*c1qbp*
atp5s	*mrpl38*	*diablo*
cmc1	*mrpl40*	*dut*
sdhaf1	*mrpl42*	*exog*
	mrps6	*fis1*
		myg1
		sco1
		timm13
		tomm34
		tomm6

[a]Transcripts with a higher expression in larvae with the 'altered' expression profile (*FDR* <0.005).

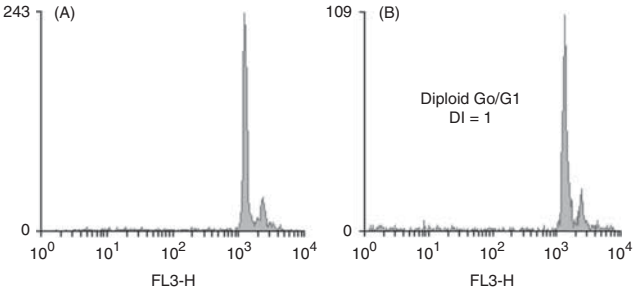

Figure 7 Nuclear DNA content from trout larvae. (A) Histogram from diploid trout progeny obtained after normal fertilization. (B) Histogram from diploid trout progeny obtained after zygotic inhibition of BER DNA repair pathway using 3AB.

reinforcing the idea that all the repairing pathways have suffered an alternative regulation. Alteration in these genes can have devastating consequences at both the cell and organism level as described by Tebbs *et al.* (1999) and Kucherlapati *et al.* (2002), who observed that targeted inactivation of enzymes acting downstream of the glycosylases in BER pathway resulted in embryonic or post-natal lethality in mice. Genes related with growth and development (at least 25 DEGs) could be responsible for the increase in malformed larvae and the increased rate of weight gain during the first 30 days. Increase in skeletal malformations could be related with a number of DEGs including those related with muscle development, such as *dmd*, *myo9b*, *tpm1*, *tpm3* (Supplementary Table 1), and the increased growth rate to the upregulation of growth factor receptors such as *igf1r* and *fgfr4* or to the downregulation of the inhibitory growth factor *ing4*.

A high number of DEGs were related with the control of cell cycle and apoptosis, suggesting a scenario of

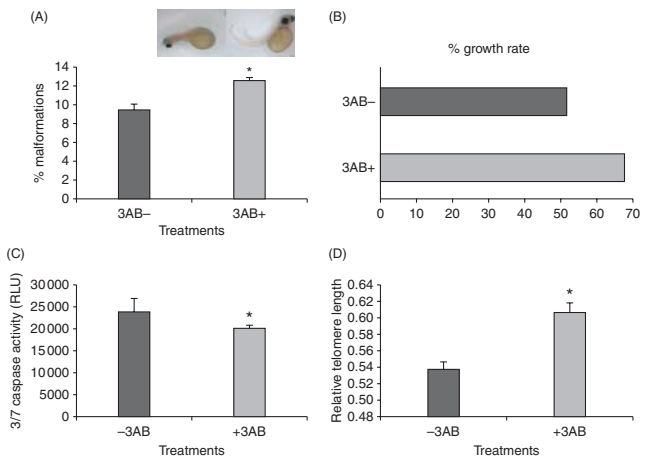

Figure 6 Malformation rates (A), weight gain from 1 to 30 dph (B), caspase 3/7 activity (C), and relative telomere length (D), in larvae obtained after normal artificial fertilization or after zygotic inhibition of BER DNA repair pathway using 3AB. Images show the most common malformations. Asterisks show significant differences between treatments ($P<0.05$).

apoptotic inhibition: *atm*, implied in the checkpoints of DNA damage and proapototic genes, *diablo*, *ddx47*, and *pttg1* are down-regulated, whereas anti-apoptotic transcripts *madd* and *igf1r* are upregulated. This down-regulation of the apoptosis was confirmed by the analysis of the caspases 3/7 activity and of the *atm*/*atr* signaling pathway, represents a source of potential mutations, and is also a mechanism allowing survival under stress conditions. The genotoxic stress promoted in the progenies was expected to generate an apoptotic response that could determine the increase in the abortion rates. Nevertheless, the analyzed larvae were able to progress with embryo development in spite of the increased genetic instability scenario. In the absence of a proper repair, residual DNA damage would lead to either apoptosis or tolerance (Menezo *et al.* 2007) and our results demonstrate that the hatched larvae actually showed a lower apoptotic activity, suggesting an increasing tolerance.

Tchernov *et al.* (2011) demonstrated that coral surviving to the thermal stress – responsible for the process of bleaching and death in reef-forming corals – are those animals in which the apoptotic cascade is downregulated. Inhibition of the apoptotic process represents a selective process preventing death under stressful conditions and boosting survival of individuals with specific characteristics.

With regard to telomere maintenance and elongation, one DEG was upregulated in treated larvae and involved in telomere maintenance, *terf1*. Downregulated DEGs have both positive (*ptges3* and *smn1*) and negative (*tcerg1*) effects on elongation. The telomere length analysis showed that the actual regulation of telomerase activity in treated larvae conduced to a higher elongation, which could be related with the impaired mechanism of DNA damage signaling of the cell cycle control and whose effects on long-term survival or aging should be analyzed.

The wide range of pathways and functions affected by the PARP inhibition could also be explained by the large number of PARP substrates, and their involvement in different regulatory activities apart from DNA repair.

PARP activity has been correlated with DNA damage since it was discovered, but modification by PARylation modulates numerous cellular processes including transcription, chromatin remodeling, apoptosis, maintenance of telomere length, etc. (Beneke 2012).

The analysis of the ploidy revealed that none of these effects are due to an interference of the inhibition treatment applied after fertilization with the mechanism of polar body extrusion, which is relatively easy to prevent in fish providing triploid animals.

Our results reinforce the importance of egg metabolism in repairing sperm DNA damage, suggesting that oocytes defective in some transcripts or proteins involved in repair could also progress with development after fertilization by damaged sperm. A reduction in DNA repair mechanisms has been described in oocytes from aged mouse (Hamatani *et al*. 2004) and other factors from genetic background to exogenous factors such as cryopreservation, *in vitro* culture, etc., could also affect the repairing activity of the zygote and compromise the long-term outcome of the progeny. In conclusion our results suggest that the oocyte has a high capacity to repair paternal DNA damage, activating more than one single repairing pathway, but long-term consequences for the progeny of any treatment affecting this repairing activity should be analyzed in depth.

Supplementary data

This is linked to the online version of the paper at http://dx.doi.org/10.1530/REP-14-0382.

Declaration of interest

The authors declare that there is no conflict of interest that could be perceived as prejudicing the impartiality of the research reported.

Funding

This work was supported by the Junta de Castilla y León (Spain) (project LE365A11-2) and the Spanish Ministry of Economy and Competitiveness (project AGL2011-27787).

Acknowledgements

The COST action FA1205 AQUAGAMETE supported a Short-Term Scientific Mission (STSM) of Cristina Fernandez-Díez at the INRA UR1037, Fish Physiology and Genomics, Rennes, France.

References

Barroso G, Valdespin C, Vega E, Kershenovich R, Avila R, Avendano C & Oehninger S 2009 Developmental sperm contributions: fertilization and beyond. *Fertility and Sterility* **92** 835–848. (doi:10.1016/j.fertnstert.2009.06.030)

Beneke S 2012 Regulation of chromatin structure by poly(ADP-ribosyl)ation. *Frontiers in Genetics* **3** 169. (doi:10.3389/fgene.2012.00169)

Bizzaro D, Manicardi G, Bianchi PG & Sakkas D 2000 Sperm decondensation during fertilisation in the mouse: presence of DNase I hypersensitive sites in situ and a putative role for topoisomerase II. *Zygote* **8** 197–202. (doi:10.1017/S0967199400000988)

Bladen CL, Lam WK, Dynan WS & Kozlowski DJ 2005 DNA damage response and Ku80 function in the vertebrate embryo. *Nucleic Acids Research* **33** 3002–3010. (doi:10.1093/nar/gki613)

Bowdin S, Allen C, Kirby G, Brueton L, Afnan M, Barratt C, Kirkman-Brown J, Harrison R, Maher ER & Reardon W 2007 A survey of assisted reproductive technology births and imprinting disorders. *Human Reproduction* **22** 3237–3240. (doi:10.1093/humrep/dem268)

Carrell DT & Hammoud SS 2010 The human sperm epigenome and its potential role in embryonic development. *Molecular Human Reproduction* **16** 37–47. (doi:10.1093/molehr/gap090)

Cartón-García F, Riesco MF, Cabrita E, Herráez MP & Robles V 2013 Quantification of lesions in nuclear and mitochondrial genes of *Sparus aurata* cryopreserved sperm. *Aquaculture* **402–403** 106–112.

Ciereszko A, Wolfe TD & Dabrowski K 2005 Analysis of DNA damage in sea lamprey (*Petromyzon marinus*) spermatozoa by UV, hydrogen peroxide, and the toxicant bisazir. *Aquatic Toxicology* **73** 128–138. (doi:10.1016/j.aquatox.2005.03.003)

Derijck AA, van der Heijden GW, Giele M, Philippens ME, van Bavel CC & de Boer P 2006 γH2AX signalling during sperm chromatin remodelling in the mouse zygote. *DNA Repair* **5** 959–971. (doi:10.1016/j.dnarep.2006.05.043)

Derijck A, van der Heijden G, Giele M, Philippens M & de Boer P 2008 DNA double-strand break repair in parental chromatin of mouse zygotes, the first cell cycle as an origin of *de novo* mutation. *Human Molecular Genetics* **17** 1922–1937. (doi:10.1093/hmg/ddn090)

Eisen MB, Spellman PT, Brown PO & Botstein D 1998 Cluster analysis and display of genome-wide expression patterns. *PNAS* **95** 14863–14868. (doi:10.1073/pnas.95.25.14863)

Evenson DP & Wixon R 2006 Clinical aspects of sperm DNA fragmentation detection and male infertility. *Theriogenology* **65** 979–991. (doi:10.1016/j.theriogenology.2005.09.011)

Fernandez-Gonzalez R, Moreira PN, Perez-Crespo M, Sanchez-Martin M, Ramirez MA, Pericuesta E, Bilbao A, Bermejo-Alvarez P, de Dios Hourcade J, de Fonseca FR *et al.* 2008 Long-term effects of mouse intracytoplasmic sperm injection with DNA-fragmented sperm on health and behavior of adult offspring. *Biology of Reproduction* **78** 761–772. (doi:10.1095/biolreprod.107.065623)

Gonzalez-Marin C, Gosalvez J & Roy R 2012 Types, causes, detection and repair of DNA fragmentation in animal and human sperm cells. *International Journal of Molecular Sciences* **13** 14026–14052. (doi:10.3390/ijms131114026)

Hamatani T, Falco G, Carter MG, Akutsu H, Stagg CA, Sharov AA, Dudekula DB, VanBuren V & Ko MS 2004 Age-associated alteration of gene expression patterns in mouse oocytes. *Human Molecular Genetics* **13** 2263–2278. (doi:10.1093/hmg/ddh241)

Hilton JF, Hadfield MJ, Tran MT & Shapiro GI 2013 Poly(ADP-ribose) polymerase inhibitors as cancer therapy. *Frontiers in Bioscience* **18** 1392–1406. (doi:10.2741/4188)

Huang da W, Sherman BT & Lempicki RA 2009 Systematic and integrative analysis of large gene lists using DAVID bioinformatics resources. *Nature Protocols* **4** 44–57. (doi:10.1038/nprot.2008.211)

Jaroudi S & SenGupta S 2007 DNA repair in mammalian embryos. *Mutation Research* **635** 53–77. (doi:10.1016/j.mrrev.2006.09.002)

Jaroudi S, Kakourou G, Cawood S, Doshi A, Ranieri DM, Serhal P, Harper JC & SenGupta SB 2009 Expression profiling of DNA repair genes in human oocytes and blastocysts using microarrays. *Human Reproduction* **24** 2649–2655. (doi:10.1093/humrep/dep224)

Kucherlapati M, Yang K, Kuraguchi M, Zhao J, Lia M, Heyer J, Kane MF, Fan K, Russell R, Brown AM *et al.* 2002 Haploinsufficiency of Flap endonuclease (Fen1) leads to rapid tumor progression. *PNAS* **99** 9924–9929. (doi:10.1073/pnas.152321699)

Lim D, Bowdin SC, Tee L, Kirby GA, Blair E, Fryer A, Lam W, Oley C, Cole T, Brueton LA *et al.* 2009 Clinical and molecular genetic features of

Beckwith–Wiedemann syndrome associated with assisted reproductive technologies. *Human Reproduction* **24** 741–747. (doi:10.1093/humrep/den406)

Lin MH, Kuo-Kuang Lee R, Li SH, Lu CH, Sun FJ & Hwu YM 2008 Sperm chromatin structure assay parameters are not related to fertilization rates, embryo quality, and pregnancy rates in *in vitro* fertilization and intracytoplasmic sperm injection, but might be related to spontaneous abortion rates. *Fertility and Sterility* **90** 352–359. (doi:10.1016/j.fertnstert.2007.06.018)

Lovato A, Panasci L & Witcher M 2012 Is there an epigenetic component underlying the resistance of triple-negative breast cancers to parp inhibitors? *Frontiers in Pharmacology* **3** 202. (doi:10.3389/fphar.2012.00202)

Marchetti F, Essers J, Kanaar R & Wyrobek AJ 2007 Disruption of maternal DNA repair increases sperm-derived chromosomal aberrations. *PNAS* **104** 17725–17729. (doi:10.1073/pnas.0705257104)

Matsuda Y & Tobari I 1989 Repair capacity of fertilized mouse eggs for X-ray damage induced in sperm and mature oocytes. *Mutation Research* **210** 35–47. (doi:10.1016/0027-5107(89)90042-0)

Menezo Y Jr, Russo G, Tosti E, El Mouatassim S & Benkhalifa M 2007 Expression profile of genes coding for DNA repair in human oocytes using pangenomic microarrays, with a special focus on ROS linked decays. *Journal of Assisted Reproduction and Genetics* **24** 513–520. (doi:10.1007/s10815-007-9167-0)

Metzger MJ, Stoddard BL & Monnat RJ Jr 2013 PARP-mediated repair, homologous recombination, and back-up non-homologous end joining-like repair of single-strand nicks. *DNA Repair* **12** 529–534. (doi:10.1016/j.dnarep.2013.04.004)

Mitra S, Boldogh I, Izumi T & Hazra TK 2001 Complexities of the DNA base excision repair pathway for repair of oxidative DNA damage. *Environmental and Molecular Mutagenesis* **38** 180–190. (doi:10.1002/em.1070)

Moussa M, Marinet V, Trimeche A, Tainturier D & Anton M 2002 Low density lipoproteins extracted from hen egg yolk by an easy method: cryoprotective effect on frozen–thawed bull semen. *Theriogenology* **57** 1695–1706. (doi:10.1016/S0093-691X(02)00682-9)

Perez-Cerezales S, Martinez-Paramo S, Beirao J & Herraez MP 2010*a* Fertilization capacity with rainbow trout DNA-damaged sperm and embryo developmental success. *Reproduction* **139** 989–997. (doi:10.1530/REP-10-0037)

Perez-Cerezales S, Martinez-Paramo S, Beirao J & Herraez MP 2010*b* Evaluation of DNA damage as a quality marker for rainbow trout sperm cryopreservation and use of LDL as cryoprotectant. *Theriogenology* **74** 282–289. (doi:10.1016/j.theriogenology.2010.02.012)

Perez-Cerezales S, Gutierrez-Adan A, Martinez-Paramo S, Beirao J & Herraez MP 2011 Altered gene transcription and telomere length in trout embryo and larvae obtained with DNA cryodamaged sperm. *Theriogenology* **76** 1234–1245. (doi:10.1016/j.theriogenology.2011.05.028)

Schulte RT, Ohl DA, Sigman M & Smith GD 2010 Sperm DNA damage in male infertility: etiologies, assays, and outcomes. *Journal of Assisted Reproduction and Genetics* **27** 3–12. (doi:10.1007/s10815-009-9359-x)

Shimura T, Inoue M, Taga M, Shiraishi K, Uematsu N, Takei N, Yuan ZM, Shinohara T & Niwa O 2002 p53-dependent S-phase damage checkpoint and pronuclear cross talk in mouse zygotes with X-irradiated sperm. *Molecular and Cellular Biology* **22** 2220–2228. (doi:10.1128/MCB.22.7.2220-2228.2002)

Smith TB, Dun MD, Smith ND, Curry BJ, Connaughton HS & Aitken RJ 2013 The presence of a truncated base excision repair pathway in human spermatozoa that is mediated by OGG1. *Journal of Cell Science* **126** 1488–1497. (doi:10.1242/jcs.121657)

Speyer BE, Pizzey AR, Ranieri M, Joshi R, Delhanty JD & Serhal P 2010 Fall in implantation rates following ICSI with sperm with high DNA fragmentation. *Human Reproduction* **25** 1609–1618. (doi:10.1093/humrep/deq116)

Tchernov D, Kvitt H, Haramaty L, Bibby TS, Gorbunov MY, Rosenfeld H & Falkowski PG 2011 Apoptosis and the selective survival of host animals following thermal bleaching in zooxanthellate corals. *PNAS* **108** 9905–9909. (doi:10.1073/pnas.1106924108)

Tebbs RS, Flannery ML, Meneses JJ, Hartmann A, Tucker JD, Thompson LH, Cleaver JE & Pedersen RA 1999 Requirement for the Xrcc1 DNA base excision repair gene during early mouse development. *Developmental Biology* **208** 513–529. (doi:10.1006/dbio.1999.9232)

Thomson LK, Fleming SD, Aitken RJ, De Iuliis GN, Zieschang JA & Clark AM 2009 Cryopreservation-induced human sperm DNA damage is predominantly mediated by oxidative stress rather than apoptosis. *Human Reproduction* **24** 2061–2070. (doi:10.1093/humrep/dep214)

Ward WS 2010 Function of sperm chromatin structural elements in fertilization and development. *Molecular Human Reproduction* **16** 30–36. (doi:10.1093/molehr/gap080)

Yamauchi Y, Shaman JA, Boaz SM & Ward WS 2007 Paternal pronuclear DNA degradation is functionally linked to DNA replication in mouse oocytes. *Biology of Reproduction* **77** 407–415. (doi:10.1095/biolreprod.107.061473)

Zhang Q & Arai K 1996 Flow cytometry for DNA contents of somatic cells and spermatozoa in the progeny of natural tetraploid loach. *Fisheries Science* **62** 870–877.

Zini A 2011 Are sperm chromatin and DNA defects relevant in the clinic? *Systems Biology in Reproductive Medicine* **57** 78–85. (doi:10.3109/19396368.2010.515704)

Zini A & Sigman M 2009 Are tests of sperm DNA damage clinically useful? Pros and cons. *Journal of Andrology* **30** 219–229. (doi:10.2164/jandrol.108.006908)

Zini A, Boman JM, Belzile E & Ciampi A 2008 Sperm DNA damage is associated with an increased risk of pregnancy loss after IVF and ICSI: systematic review and meta-analysis. *Human Reproduction* **23** 2663–2668. (doi:10.1093/humrep/den321)

Received 30 July 2014
First decision 21 August 2014
Revised manuscript received 2 October 2014
Accepted 27 October 2014